

## SECURE IDENTIFICATION OF FREE-FLOATING PLANETS

CHEONGHO HAN

Department of Physics, Institute for Basic Science Research, Chungbuk National University, Chongju 361-763, Korea;  
cheongho@astroph.chungbuk.ac.kr  
Draft version September 28, 2018

### ABSTRACT

Among the methods proposed to detect extrasolar planets, microlensing is the only technique that can detect free-floating planets. Free-floating planets are detected through the channel of short-duration isolated lensing events. However, if a seemingly isolated planetary event is detected, it is difficult to firmly conclude that the event is caused by a free-floating planet because a wide-separation planet can also produce an isolated event. There were several methods proposed to break the degeneracy between the isolated planetary events produced by the free-floating and wide-separation planets, but they are incomplete. In this paper, we show that free-floating planets can be securely identified by conducting astrometric follow-up observations of isolated events to be detected in future photometric lensing surveys by using high-precision interferometers to be operated contemporarily with the photometric surveys. The method is based on the fact that astrometric lensing effect covers much longer range of the lens-source separation than the photometric effect. We demonstrate that several astrometric follow-up observations of isolated planetary events associated with source stars brighter than  $V \sim 19$  by using the *Space Interferometry Mission* with an exposure time of  $\lesssim 10$  min for each observation will make it possible to measure the centroid shift induced by primaries with projected separations up to  $\sim 100$  AU. Therefore, the proposed method is far more complete than previously proposed methods that are flawed by the limited applicability only to planets with projected separations  $\lesssim 20$  AU or planets accompanied by bright primaries.

*Subject headings:* gravitational lensing – planets and satellite: general

### 1. INTRODUCTION

Although originally proposed as a method to search for Galactic dark matter in the form of massive compact objects (Paczynski 1986), microlensing has developed into important tools in various aspects of astrophysics (see the review Gould 2001), including the detection and characterization of extrasolar planets (Mao & Paczynski 1991). Recently, three robust microlensing detections of exoplanets were reported by Bond et al. (2004), Udalski et al. (2005), and Beaulieu et al. (2006).

The microlensing signal of a planet is a short-duration perturbation to the smooth standard light curve of the primary-induced lensing event occurring on a background source star. The planetary lensing signal induced by a giant planet with a mass equivalent to that of the Jupiter lasts for a duration of  $\sim 1$  day, and the duration decreases in proportion to the square root of the mass of a planet, reaching several hours for an Earth-mass planet. To achieve the observational frequency required to detect the short-lived planetary signal, current microlensing planet search experiments are operated in a special observational setup, where survey observations issue alerts of ongoing events in the early stage of lensing magnification (Udalski et al. 1994; Alcock et al. 1997; Bond et al. 2001) and follow-up observations intensively monitor the alerted events (Albrow et al. 1998; Yoo et al. 2004). However, follow-up is generally done with an instrument having a small field of view, and thus events should be monitored in sequence. As a result, only a handful number of events can be followed at any given time, and thus the number of planet detections is limited.

However, the situation will be different in next-generation lensing experiments that will survey wide fields continuously at high cadence by using very large-format imaging cameras. Several such surveys in space and on the ground have al-

ready been proposed or are being seriously considered. The *Galactic Exoplanet Survey Telescope (GEST)*, whose concept was succeeded by the *Microlensing Planet Finder (MPF)*, is a space mission to be equipped with a 1–2 m aperture telescope (Bennett & Rhie 2002; Gould 2005). The ‘Earth-Hunter’ project is a ground-based survey that plans to achieve  $\sim 10$  minute sampling by using a network of three 2 m class wide-field ( $\sim 2^\circ \times 2^\circ$ ) telescopes scattered over the southern hemisphere (A. Gould, private communication). These next-generation surveys dispense with the alert/follow-up mode of searching for planets, and instead simultaneously obtain densely-sampled lightcurves of all microlensing events in their field-of-view, yielding improved sensitivity to planets.

In addition to the dramatically improved sensitivity to planets, the next-generation lensing surveys can detect two new populations of wide-separation and free-floating planets (Bennett & Rhie 2002; Han et al. 2004, 2005). In the current planet search strategy based on alert/follow-up mode, events can be followed only when the source star is located within the Einstein ring of the primary lens. Such source positions are only sensitive to planets located within a certain range of distance from their host stars (Gould & Loeb 1992). Planets in this so-called lensing zone have separations in the range of  $0.6 \lesssim s \lesssim 1.6$ , where  $s$  is the projected star-planet separation normalized by the Einstein radius  $r_E$ . The Einstein radius is related to the mass of the lens (i.e., the host star of the planet)  $m$  and distances to the lens  $D_L$  and source (background lensed star)  $D_S$  by

$$r_E \simeq 4.9 \text{ AU} \left( \frac{m}{0.5 M_\odot} \right)^{1/2} \left( \frac{D_L}{6 \text{ kpc}} \right)^{1/2} \left( 1 - \frac{D_L}{D_S} \right)^{1/2}. \quad (1)$$

For a typical Galactic bulge event caused by a low-mass stellar lens with  $m = 0.5 M_\odot$ ,  $D_L = 6$  kpc, and  $D_S = 8$  kpc, the Einstein radius is  $r_E \sim 2.5$  AU. Therefore, current microlensing planet

search strategy is sensitive only to *bound* planets in the range of the projected separation of  $1 \text{ AU} \lesssim r_{\perp} \lesssim 5 \text{ AU}$ . In the future survey, however, events will be monitored regardless of whether the primary of a planet magnifies the background source star or not, and thus wide-separation and free-floating planets can be detected through the channel of *isolated* events.

Among the two new populations of planets to be detected in the future lensing surveys, free-floating planets are of special interest. Most theories of planet formation predict that a large number of planets are ejected from their planetary systems during or after the epoch of their formation. However, it would be difficult to test these theories without a capacity to detect the free-floating planets arising from such ejections. The importance of microlensing detections of free-floating planets lies in the fact that microlensing is the only proposed method that can detect these planets. All other techniques rely on the effect of the planet on its parent star (either jostling the star's position or blocking its light), and thus they can detect only planets that are bound to their parent stars.

However, there is a problem in identifying free-floating planets. The problem is that both the free-floating and wide-separation planets exhibit their existence through the same channel of isolated events. Han et al. (2005) proposed three methods for distinguishing isolated events caused by the two populations of planets. These include detecting the primary through the influence of the planetary caustic, through the low-amplitude bump in the lightcurve from the primary, and through the detection of the light from the primary itself (see § 3 for details). However, a substantial fraction of events caused by wide-separation planets do not show symptoms of their primaries, and thus they cannot be distinguished from those produced by free-floating events. As a result, if a seemingly isolated planetary event is detected, it is difficult to firmly conclude that the event is caused by a free-floating planet.

In addition to photometric observations, microlensing events can also be observed astrometrically by using future high-precision interferometers such as those to be mounted on space-based platforms, e.g. the *Space Interferometric Mission (SIM)* and the *Global Astrometric Interferometers for Astrophysics (GAIA)*, and those to be mounted on very large ground-based telescopes, e.g. Keck and VLT. If an event is astrometrically observed by using these instruments, it is possible to measure the lensing-induced positional displacement of the centroid of the source star image with respect to its unlensed position (Høg, Novikov, & Polnarev 1995; Miyamoto & Yoshii 1995; Walker 1995; Paczyński 1998; Boden, Shao, & Van Buren 1998; Han & Kim 1999). Recently, the proposal of astrometric microlensing observations was selected as one of the long-term projects of the *SIM*, which is scheduled to be launched in 2013. Then, a significant time of the next-generation photometric lensing surveys will overlap with that of the *SIM* observations, and thus astrometric follow-up observations of events detected from the photometric surveys will be possible in the future. In this paper, we demonstrate that astrometric follow-up observations of an isolated planetary lensing event by using high-precision interferometers can firmly distinguish whether the event is produced by a wide-separation planet or a free-floating planet.

The paper is organized as follows. In § 2, we briefly describe basics of photometric and astrometric behaviors of microlensing events. In § 3, we mention about the previously proposed methods to break the degeneracy between the isolated planetary lensing events caused by wide-separation and free-floating planets and discuss the limitations of the meth-

ods. In § 4, we describe the basic scheme of the proposed method and demonstrate the feasibility of the method. We also discuss the superiority of the proposed method over the previously proposed methods. In § 5, we summarize and conclude.

## 2. BASICS OF PHOTOMETRIC AND ASTROMETRIC LENSING

A planetary lensing is described by the formalism of a binary lensing with a very low-mass companion. For binary lensing, the mapping from the lens plane to the source plane is expressed as

$$\zeta = z - \sum_{j=1}^2 \frac{m_j/m}{\bar{z} - \bar{z}_{L,j}}, \quad (2)$$

where  $\zeta = \xi + i\eta$ ,  $z_{L,j} = x_{L,j} + iy_{L,j}$ , and  $z = x + iy$  are the complex notations of the source, lens, and image positions, respectively,  $\bar{z}$  denotes the complex conjugate of  $z$ ,  $m_j$  are the masses of the individual lens components, and  $m = m_1 + m_2$  (Witt 1990). Here all angles are normalized to the angular size of the Einstein radius of the total mass of the system, i.e.

$$\theta_E = \frac{r_E}{D_L} \simeq 710 \mu\text{as} \left( \frac{m}{0.5 M_{\odot}} \right)^{1/2} \left( \frac{D_S}{8 \text{ kpc}} \right)^{-1/2} \left( \frac{D_S}{D_L} - 1 \right)^{1/2}. \quad (3)$$

The lensing process conserves the source surface brightness, and thus the magnifications  $A_i$  of the individual images correspond to the ratios between the areas of the images and the source. For an infinitesimally small source element, the magnification is mathematically expressed as

$$A_i = \left| \left( 1 - \frac{\partial \zeta}{\partial \bar{z}} \frac{\partial \bar{\zeta}}{\partial z} \right)^{-1} \right|. \quad (4)$$

Then the total magnification is sum of the magnifications of the individual images,  $A = \sum_i A_i$ . The position of the image centroid corresponds to the magnification weighted mean position of the individual images, and thus the displacement of the position of the source star image centroid with respect to its unlensed position (centroid shift) is expressed as

$$\boldsymbol{\delta} = \left( \frac{\sum A_i \mathbf{z}_i}{A} - \boldsymbol{\zeta} \right) \theta_E, \quad (5)$$

where  $\boldsymbol{\zeta}$  and  $\mathbf{z}_i$  are the vector notations of the source and image positions, respectively.

Because of the very small mass ratio, planetary lensing behavior is well described by that of a single lens of the primary star for most of the event duration. The single-lens magnification and centroid shift vector of the source star image are expressed respectively as

$$A = \frac{u^2 + 2}{u(u^2 + 4)^{1/2}}, \quad (6)$$

$$\boldsymbol{\delta} = \frac{\mathbf{u}}{u^2 + 2} \theta_E, \quad (7)$$

where  $\mathbf{u}$  is the dimensionless lens-source separation vector normalized by  $\theta_E$ . The lightcurve of a single-lens event is characterized by a smooth and symmetric shape. The trajectory of the centroid shift traces an ellipse with a minor/major axis ratio of  $b/a = u_0/(u_0^2 + 2)^{1/2}$ , where  $u_0$  is the impact parameter of the lens-source encounter normalized by  $\theta_E$ . Due to the existence of the planet, however, a short-duration perturbation can occur when the source star passes the region

around the caustics, which represent the set of source positions at which the magnification of a point source becomes infinite. For a planetary case, there exist two sets of disconnected caustics. One small central caustic is located close to the host star and the other bigger planetary caustic is located away from the host star. For a wide-separation planet, the planetary caustic has an asterisk shape with four cusps, where two of them are located on the star-planet axis and the other two are off the axis. The center of the planetary caustic is located at

$$\mathbf{r}_c = \mathbf{s} \left( 1 - \frac{1}{s^2} \right), \quad (8)$$

where  $\mathbf{s}$  is the position vector of the planet from the star normalized by the Einstein radius. The caustic size, which is directly proportional to the cross-section of the planetary perturbation, as measured by the full width along the star-planet axis and a height normal to the star-planet axis are

$$\Delta\xi_c \simeq \frac{4q^{1/2}}{s\sqrt{s^2-1}}, \quad \Delta\eta_c \simeq \frac{4q^{1/2}}{s\sqrt{s^2+1}}, \quad (9)$$

where  $q$  is the planet/star mass ratio. For details about the location, shape, and size of the caustic, see Han (2006). Then, as the separation between the star and planet increases, the position of the caustic moves toward the position of the planet itself ( $\mathbf{r}_c \rightarrow \mathbf{s}$ ) and the size of the caustic rapidly decreases as  $\Delta\xi$  ( $\Delta\eta$ )  $\propto s^{-2}$ . As a result, a wide-separation planet ( $s \gg 1$ ) behaves as if it is an independent lens. Therefore, the lightcurve of an event with source trajectory passing through the effective region of the wide-separation planet appears to be that of a single-lens event produced by a free-floating planet.

### 3. PREVIOUS METHODS

There are several methods that were proposed to identify the existence of the primary star in isolated events caused by wide-separation planets, and thus enabling discrimination between bound and free-floating planets. The first method is detecting the signature of the primary stars near the peak of lightcurves. The signature is produced by the planetary caustic, which is located at the center of the effective lensing position of the planet. With this method, it was estimated that primary signatures with  $\gtrsim 5\%$  photometric deviation can be detected for  $\gtrsim 80\%$  of isolated events (with source trajectories approaching within the Einstein ring of the planet,  $\theta_{E,p} = q^{1/2}\theta_E$ ) caused by Jupiter-mass planets with projected separations  $r_\perp \lesssim 10$  AU (Han & Kang 2003). However, the caustic shrinks rapidly with the increase of the planet separation as  $\propto s^{-2}$ , and thus the chance to detect the primary signature also decreases accordingly. Therefore, considering that nearly one third of planets in our solar system have separations of  $\gtrsim 20$  AU, this method is significantly incomplete in distinguishing between bound and free-floating planets.

Second, wide-separation planetary events can also be distinguished by the additional long-term bumps in the lightcurve caused by the primary star. Compared to the planetary Einstein ring, the Einstein ring of the primary star is much larger, and thus the source trajectory passing through the region around the planet has a good chance to approach the effective lensing region of the primary. Han et al. (2005) estimated that with this method the existence of the primary can be identified for  $\gtrsim 50\%$  of events with  $r_\perp \lesssim 20$  AU. However, the chance to detect the bump decreases linearly with the

increase of the planetary separation, and thus this method is also incomplete.

The third method of identifying a wide-separation planet is detecting blended light from the host star. This method is possible because photometry of the proposed space-based microlensing mission will not be affected by the blended flux from stars located close to the lensed source star thanks to high resolution from space observation combined with the fact that the main target source stars of the mission are low-luminosity main-sequence stars for which the lens/source flux ratio is relatively high. According to Bennett & Rhie (2002), for  $\sim 1/3$  of events with detected planets from a space lensing mission, the planetary host star is either brighter than or within  $\sim 2$  magnitudes of the source star's brightness. This method has an advantage that primary detection is possible regardless of the planetary separation, but it has a disadvantage that it cannot be applicable to events associated with faint or dark primaries.

### 4. NEW METHOD: ASTROMETRIC FOLLOW-UP

In this section, we demonstrate that astrometric follow-up observations of isolated planetary lensing events by using high-precision interferometers can firmly break the degeneracy in the events produced by wide-separation and free-floating planets. The method is based on the fact that astrometric lensing effect covers much longer range of lens-source separation than photometric effect (Miralda-Escudé 1996). In the limiting case of  $u \gg 1$ , the astrometric and photometric effects are approximated respectively as

$$A \rightarrow 1 + \frac{2}{u^4}, \quad (10)$$

$$\delta \rightarrow \frac{\theta_E}{u}. \quad (11)$$

Therefore, the photometric effect vanishes rapidly as  $\propto u^{-4}$ , while the astrometric effect decays much more slowly as  $\propto u^{-1}$ . Then, for an isolated event produced by a wide-separation planet, the astrometric effect of the primary will be considerable although its photometric effect is negligible.

In Figure 1, we illustrate the basic scheme of the method. In the main panel of the figure, we present the geometry of isolated planetary events produced by wide-separation planets with various distances from the primary. The coordinates are centered at the effective position of the planet. The effective planet position is located at a position with a separation  $1/s$  from the planet toward the primary and it corresponds to the center of the planetary caustic. For the physical parameters of the lens system, we assume that the mass of the lens is  $m = 0.5 M_\odot$  and the distances to the lens and source stars are  $D_L = 6$  kpc and  $D_S = 8$  kpc, respectively, by adopting the values of a typical Galactic bulge event. We assume that the planet/primary mass ratio is  $q = 3 \times 10^{-3}$ . The primaries are located on the left side of the planet with normalized separations of  $s = 10, 20,$  and  $30$ . In physical units, these separations correspond to the projected separations of  $r_\perp = 24.7$  AU,  $49.4$  AU, and  $74.1$  AU, respectively. The positions of the individual primary stars are marked by crosses with blue (also marked by number '1'), red ('2'), and green ('3') colors and the dashed circles around the individual primaries represent the Einstein rings of the primaries. The straight line with an arrow represents the source trajectory. The inset on the upper right side shows the enlarged view of the region around the planet [corresponding to the region inside the dotted square

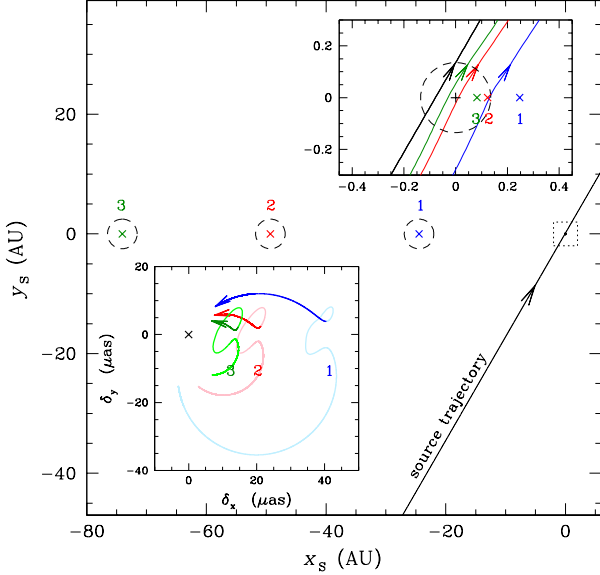


FIG. 1.— The geometry of isolated planetary events produced by wide-separation planets with various distances from the primary (main panel) and the resulting trajectories of the source star image centroid shifts (lower left inset). The inset on the upper right side shows the enlarged view of the region around the planet [corresponding to the region inside the dotted square centered on (0,0) in the main panel]. See detailed explanation in text.

centered on (0,0) in the main panel], where the dashed circle is the Einstein ring of the planet, the black straight line is the source trajectory, and the crosses and curves drawn in colors represent the true positions of the planets and the trajectories of the source star image centroid for the three cases of lens system geometry with primaries located at the positions marked by the corresponding colors (and numbers). The inset on the lower left side shows the trajectories of the centroid shifts of the events produced by the individual primary-planet pairs. Each trajectory is drawn in two tones of color, where the part drawn in the dark-tone color indicates the trajectory after the planetary lensing event, while the light-tone part indicates the trajectory before and during the event. Since astrometric follow-up observations will be carried out after the event, the dark-tone part of the trajectory is what will be observed.

From the figure, we find the following trends of centroid shifts.

1. Due to the much larger size of the Einstein ring of the primary, the centroid motion is dominated by the astrometric effect of the primary in most of the time of the centroid motion. Since the source trajectory has a large impact parameter with respect to the primary, i.e.  $u_0 \gg 1$ , the minor/major axis ratio of the primary-induced centroid shift trajectory is  $b/a = u_0/(u_0^2 + 2)^{1/2} \rightarrow 1$ , and thus the trajectory has a circular shape.
2. The astrometric effect of the planet becomes equivalent to or larger than that of the primary in the region where  $d_{\perp,p} \lesssim qd_{\perp,*}$ . Here  $d_{\perp,p}$  and  $d_{\perp,*}$  represent the projected distances from the source to the planet and primary star, respectively. As a result, during the time when the source is located within this region, the centroid shift trajectory deviates from the circular one induced by the primary. However, due to the small mass

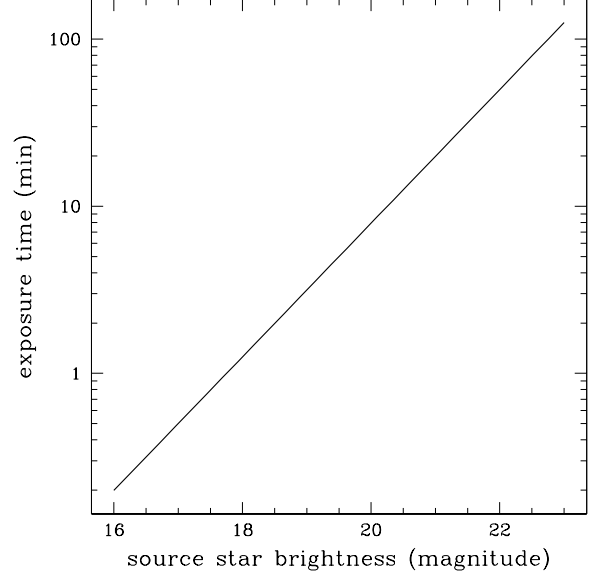


FIG. 2.— The *SIM* exposure time required to achieve positional accuracy better than a threshold value  $\delta_{\text{th}} = 4 \mu\text{as}$  as a function of source brightness. The threshold value corresponds to the amount of the centroid shift caused by a primary star of a wide-separation planetary system with a projected separation of  $r_{\perp} = 100 \text{ AU}$  from the planet.

ratio of the planet, the deviation lasts only a short period of time. The planet-induced perturbation traces an elliptical trajectory with an axis ratio of  $u_{0,p}/(u_{0,p}^2 + 2)^{1/2}$ , where  $u_{0,p}$  is the planet-source impact parameter normalized by the Einstein radius of the planet. Therefore, if the source passes closer to (further from) the effective planet position than the case shown in Figure 1, the part of the elliptical trajectory induced by the planet would be more elongated (circular). However, this shift of the source trajectory has little effect on the source-primary separation, and thus the part of the centroid shift trajectory induced by the primary remains nearly the same.

3. Despite the large separation between the primary and the source near the planet, the centroid shift induced by the primary is substantial. The amount of the primary-induced centroid shift is

$$\delta \simeq 40 \mu\text{as} \left( \frac{\theta_E}{410 \mu\text{as}} \right) \left( \frac{r_{\perp}}{10 \text{ AU}} \right)^{-1}. \quad (12)$$

Then, a question is how well the astrometric signature of primaries can be measured by the *SIM* observations. According to the specification of the *SIM*, it will have positional accuracy of  $\sigma \sim 0.4 \mu\text{as}$  for a star of  $V = 12$  with an exposure time of  $t_{\text{exp}} = 0.5 \text{ min}$  and the uncertainty increases with the decrease of the photon count. According to equation (12), the threshold centroid shift to identify the existence of primaries with separations up to  $r_{\perp} \sim 100 \text{ AU}$  is  $\delta_{\text{th}} \sim 4 \mu\text{as}$ . Then, the exposure time required to achieve astrometric accuracy to measure the threshold centroid shift is

$$t_{\text{exp}} \simeq 0.08 \text{ min} \left( \frac{\delta_{\text{th}}}{4 \mu\text{as}} \right)^{-2} 10^{0.4(V-12)}, \quad (13)$$

where  $V$  is the source star magnitude. In Figure 2, we present the required exposure time as a function of source star brightness. The exposure time in equation (13) is based on photon

noise. However, even considering other sources of noise, it will be possible to measure centroid shift of  $\delta > \delta_{\text{th}}$  for events involved with source stars brighter than  $V \sim 19$  with exposure times of  $t_{\text{exp}} \lesssim 10$  min. Therefore, by focusing on isolated events associated with bright source stars, astrometric follow-up observations can be carried out not seriously affecting the *SIM* lensing observations for its original goal. In addition, the centroid motion is slow when the source is away from the primary, and thus follow-up does not require prompt response just after the planetary lensing.

Compared to the previous astrometric methods, the proposed method has the following important advantages. First, the proposed method is complete in the sense that it can identify the bound nature of nearly all planets within the possible range of distance ( $\lesssim 100$  AU) from the primary. Second, the astrometric effect of the primary does not depend on brightness of the primary, and thus the proposed method can be applied to planets accompanied with faint or even dark primaries. Third, astrometric observation of the primary-induced centroid shift enables one to measure the angular Einstein ring radius. While the Einstein timescale, which is determined from photometric observation, results from the combination of the three physical parameters of the lens mass, distance to the lens, and lens-source transverse speed,  $\theta_E$  does not depend on the transverse speed. Therefore, one can better constrain the mass of the primary, and thus that of the planet.

## 5. CONCLUSION

We showed that free-floating planets can be securely identified by conducting astrometric follow-up observations of isolated events to be detected in future photometric lensing surveys by using high-precision interferometers to be operated contemporarily with the photometric surveys. The method is based on the fact that astrometric lensing effect covers much longer range of the lens-source separation than the photometric effect. We demonstrated that several astrometric follow-up observations of isolated planetary events associated with source stars brighter than  $V \sim 19$  by using the *Space Interferometry Mission* with an exposure time of  $\lesssim 10$  min for each observation will make it possible to measure the centroid shift induced by primaries with projected separations up to  $\sim 100$  AU. Therefore, the proposed method is far more complete than previously proposed methods that are flawed by the limited applicability only to planets with projected separations  $\lesssim 20$  AU or planets accompanied by bright primaries.

This work was supported by the Astrophysical Research Center for the Structure and Evolution of the Cosmos (ARCSEC) of the Korea Science & Engineering Foundation (KOSEF) through the Science Research Program (SRC) program.

## REFERENCES

- Albrow, M., et al. 1998, *ApJ*, 509, 687  
 Alcock, C., et al. 1997, *ApJ*, 491, 436  
 Beaulieu, J.-P., et al. 2006, *Nature*, 439, 437  
 Bennett, D. P., & Rhie, S. H. 2002, *ApJ*, 574, 985  
 Bond, I. A., et al. 2001, *MNRAS*, 327, 868  
 Bond, I. A., et al. 2004, *ApJ*, 606, L155  
 Boden, A. F., Shao, M., & Van Buren, D. 1998, *ApJ*, 502, 538  
 Gould, A. 2001, *PASP*, 113, 903  
 Gould, A. 2005, *New Astronomy Reviews*, 49, 424  
 Gould, A., & Loeb, A. 1992, *ApJ*, 396, 104  
 Han, C. 2006, *ApJ*, 638, 1080  
 Han, C., Chung, S.-J., Kim, D., Park, B.-G., Ryu, Y.-H., Kang, S., & Lee, D. 2004, *ApJ*, 604, 372  
 Han, C., & Kang, Y. W. 2003, *ApJ*, 596, 1320  
 Han, C., & Kim, T.-W. 1999, *MNRAS*, 305, 795  
 Han, C., Gaudi, B. S., An, J. H., & Gould, A. 2005, *ApJ*, 618, 962  
 Høg, E., Novikov, I. D., & Polnarev, A. G. 1995, *A&A*, 294, 287  
 Mao, S., & Paczyński, B. 1991, *ApJ*, 374, L37  
 Miral-Escude, J. 1996, *ApJ*, 470, L113  
 Miyamoto, M., & Yoshii, Y. 1995, *AJ*, 110, 1427  
 Paczyński, B. 1986, *ApJ*, 304, 1  
 Paczyński, B. 1998, *ApJ*, 494, L23  
 Udalski, A., et al. 2005, *ApJ*, 628, L109  
 Udalski, A., Szymański, M., Kałużny, J., Kubiak, M., Mateo, M., Krzemiński, W., & Paczyński, B. 1994, *Acta Astron.*, 44, 227  
 Walker, M. A. 1995, *ApJ*, 453, 37  
 Witt, H. J. 1990, *A&A*, 236, 311  
 Yoo, J., et al. 2004, *ApJ*, 616, 1204